

Side Reactions of Nitroxide-Mediated Polymerization: N–O versus O–C Cleavage of Alkoxyamines

Jennifer L. Hodgson,[†] Luke B. Roskop,[‡] Mark S. Gordon,[‡] Ching Yeh Lin,[†] and Michelle L. Coote^{*,†}

Australian Research Council Centre of Excellence for Free Radical Chemistry and Biotechnology, Research School of Chemistry, Australian National University, Canberra, ACT 0200, Australia, and Department of Chemistry, Iowa State University, Ames, Iowa 50011

Received: July 12, 2010; Revised Manuscript Received: August 18, 2010

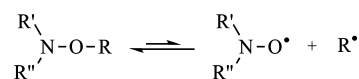
Free energies for the homolysis of the NO–C and N–OC bonds were compared for a large number of alkoxyamines at 298 and 393 K, both in the gas phase and in toluene solution. On this basis, the scope of the N–OC homolysis side reaction in nitroxide-mediated polymerization was determined. It was found that the free energies of NO–C and N–OC homolysis are not correlated, with NO–C homolysis being more dependent upon the properties of the alkyl fragment and N–OC homolysis being more dependent upon the structure of the aminyl fragment. Acyclic alkoxyamines and those bearing the indoline functionality have lower free energies of N–OC homolysis than other cyclic alkoxyamines, with the five-membered pyrrolidine and isoindoline derivatives showing lower free energies than the six-membered piperidine derivatives. For most nitroxides, N–OC homolysis is normally favored above NO–C homolysis only when a heteroatom that is α to the NOC carbon center stabilizes the NO–C bond and/or the released alkyl radical is not sufficiently stabilized. As part of this work, accurate methods for the calculation of free energies for the homolysis of alkoxyamines were determined. Accurate thermodynamic parameters to within 4.5 kJ mol^{−1} of experimental values were found using an ONIOM approximation to G3(MP2)-RAD combined with PCM solvation energies at the B3-LYP/6-31G(d) level.

1. Introduction

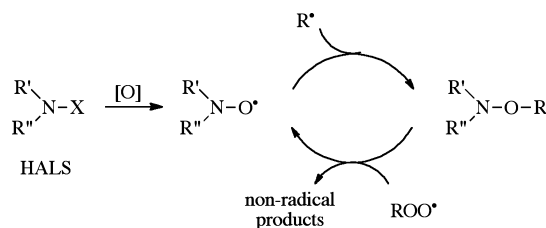
The dissociation of an alkoxyamine into a nitroxide radical and an alkyl radical (Scheme 1) as well as the reverse, a combination reaction of these two species, is central to many industrially relevant processes. These types of reactions are important when nitroxides are utilized as radical traps, as control agents in radical polymerization, and as stabilizers of polymer coatings. The control reaction of nitroxide-mediated polymerization (NMP) involves the reversible trapping of a growing polymer chain by a nitroxide to form a dormant alkoxyamine, thereby preventing uncontrolled chain growth. A similar trapping reaction also makes up part of the Denisov cycle, which involves the catalytic protection of polymer coatings against photo-oxidative damage by hindered amine light stabilizers (HALS) (Scheme 2).^{1,2}

When alkoxyamines are used in NMP and also when they are formed from hindered amine light stabilizers as part of the Denisov cycle, competition exists in the homolysis of alkoxyamines between the desired dissociation at the NO–C bond and the dissociation at the N–OC bond. N–OC homolysis occurs as an unwanted side reaction, leading to the formation of aminyl radicals and highly reactive and possibly polymer-damaging free alkoxy radicals. An understanding of the effects of the chemical structure of the nitroxide and the propagating radical on the competition between these two processes would therefore be extremely useful. In particular, it would assist in the design and selection of nitroxides that were more resistant to the unwanted N–OC homolysis process.

SCHEME 1: Reversible Homolysis of Alkoxyamine at the R'R''NO–R Bond, Forming the Control Reaction for Nitroxide-Mediated Polymerization



SCHEME 2: Simplified Mechanism of the Denisov Cycle, Showing Protection Using a Piperidine HALS (where X is typically H or an alkyl chain)



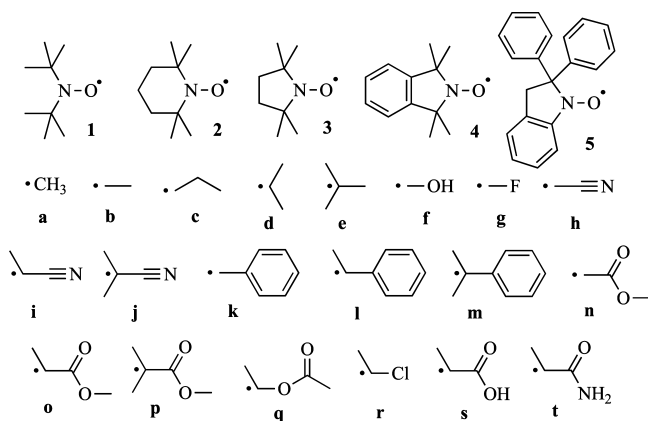
Previously, this competition has been studied by Siri et al.³ and Gimes et al.⁴ for several piperidine- and indoline-based alkoxyamines using density functional theory (DFT) as well as experimental methods. The main finding for the piperidine-ring systems was that NO–C homolysis has lower bond dissociation energies (BDEs) than N–OC except in the case of a vinyl acetate monomer-substituted alkoxyamine, which had an NO–C bond stabilized by an anomeric interaction. For the studied indoline alkoxyamines, it was concluded that N–OC homolysis was preferred except for alkoxyamines substituted with an C(CH₃)₂CO₂CH₂CH₃ alkyl fragment. However, it would be useful to extend this study to include a larger range of alkyl fragments as well as acyclic and other common cyclic nitroxide species.

* Corresponding author. E-mail: mcoote@rsc.anu.edu.au.

[†] Australian National University.

[‡] Iowa State University.

SCHEME 3: Nitroxide and Alkyl Radical Species in This Study Formed by the NO–C Bond Homolysis of Alkoxyamines



Additionally, in these previous studies,^{3,4} it was found that the DFT and semiempirical methods used showed large variations from each other and from the experimental BDEs, although the DFT methods were able to model the NO–C versus N–OC competition successfully. Elsewhere, we have shown that a variety of DFT methods failed to model even the qualitative trends in NO–C BDEs of a series of alkoxyamines.⁵ Although it is expected that the DFT methods used in these previous studies may provide a reasonable measure of the difference in BDEs for NO–C and N–OC bond homolysis, it is likely that higher-level calculations will be required for the quantitative measurement of these BDEs and an understanding of structure–reactivity trends within a series.

In the present work, we use high-level *ab initio* molecular orbital calculations to examine the effects of chemical structure on the NO–C and N–OC bond dissociation energies for a broad range of alkoxyamines, with a view to predicting when the N–OC breaking side reaction is likely to be important in NMP and other applications. The various alkoxyamines in this study are illustrated by the set of nitroxide and alkyl radicals formed by the NO–C bond homolysis of alkoxyamines shown in Scheme 3. They include five- and six-membered cyclic alkoxyamines as well as acyclic species, with the alkyl fragments designed to provide models of common polymeric chains. As part of this work, we also conduct an assessment study with the aim of identifying and benchmarking reliable theoretical procedures for studying this process.

2. Theoretical Procedures

Standard *ab initio* molecular orbital⁶ and density functional⁷ calculations in this work were carried out using Gaussian 03,⁸ MOLPRO 2000.6,⁹ and GAMESS.¹⁰ Calculations on radicals were performed with an unrestricted wave function except in cases designated with an R prefix where a restricted open-shell wave function was used.

To find a suitable procedure with which to model the homolysis of alkoxyamines, the performance of a variety of levels of theory was assessed for a set of reactions for which experimental kinetic and thermodynamic parameters have been determined. Accurate methods for the calculation of geometries, gas-phase single-point energies, and free energies of solvation were determined, and the calculated equilibrium constant of the reaction was compared with experimental results. Geometries were optimized using various methods and basis sets, and the results were benchmarked against the high-level QCISD/6-

31G(d) method. To assess the effect of the level of theory used for geometry optimization on the resulting trapping enthalpies, single-point energy calculations were then carried out on all the geometries at a consistent level of theory, the QCISD/6-31G(d) level.

Gas-phase enthalpies for the trapping of several different small carbon-, oxygen-, and nitrogen-centered radical species were calculated using very high level composite methods from the W1,¹¹ CBS,¹² G4,¹³ and G3^{14,15} families and compared with experimental enthalpies in order to determine an accurate method for the calculation of gas-phase single-point energies. Enthalpies for the trapping of several different alkyl radical species by the nitroxide 2,2,6,6-tetramethylpiperidin-1-yloxy (TEMPO), using species optimized at the B3-LYP/6-31G(d) level, were calculated over a wide variety of levels of theory to determine suitable lower-cost methods for larger systems. The methods assessed include a variety of DFT methods, RMP2, and several ONIOM-type¹⁶ methods. In ONIOM, a chemical reaction is divided into a core section that includes the reaction center and principal substituents and an outer section, which is the rest of the chemical system. The core system is calculated at a high level of theory and also at a lower level of theory, but the full chemical system is calculated only at the lower level. We have previously shown that this method is suitable for reactions involving nitroxides.^{5,17–19} Three lower-cost methods were tested for the calculation of the full system in the ONIOM calculations (RMP2/6-311+G(3df,2p), BMK/6-311+G(3df,2p), and B3-LYP/6-311+G(3df,2p)), and G3(MP2)-RAD was the high level of theory used to study the core section.

The free energy of solvation, ΔG_{solv} , quantifies the free-energy difference between a gas-phase system and the same system in a solvent medium. Several procedures for the evaluation of the free energy of solvation were examined. These included polarized continuum models PCM²⁰ and CPCM,²¹ as implemented in the Gaussian 03 software package.⁸ These were employed at both the HF/6-31G(d) and B3-LYP/6-31G(d) levels of theory using the recommended radii for these calculations (i.e., the united atom topological model applied to radii optimized for the HF/6-31G(d) and PBE0/6-31G(d) levels of theory, respectively).²² For these calculations, the molecular structures of all species were reoptimized in the presence of the solvent field. In addition, free energies of solvation were also computed using the COSMO-RS²³ model, a method that describes the interactions in a fluid as local interactions of molecular surfaces. COSMO-RS free energies of solvation were calculated on gas-phase geometries via the ADF package,²⁴ using the Becke–Perdew (BP86) functional and triple- ζ -quality basis sets augmented by one set of polarization functions (TZP). Default values were used for the parameters describing the atomic cavity radii, the radius of the probing sphere, and the cavity construction.

In addition to studying the thermodynamics of the homolysis reactions, we also calculated the full reaction pathway for a model system to examine whether kinetics should follow thermodynamics. For this purpose, multiconfigurational self-consistent field (MCSCF) wave functions were constructed and single-point energies along the path were calculated at the MRMP2/6-31G(d)//FORS-MCSCF(2,2)/6-31G(d) level for both NO–C and N–OC homolysis of the 1-isopropyl-2,2,6,6-tetramethyl-piperidine (TEMPOCH(CH₃)₂) species. This level of theory is a multireference second-order perturbative treatment of orbitals initially optimized using a multiconfigurational self-consistent wave function of the fully optimized reaction space type. The T_1 diagnostic values²⁵ for the various species along

this path were also determined. So as to facilitate the calculation of thermal and entropic corrections, frequencies along these reaction paths were calculated at the FORS-MCSCF(2,2)/6-31G(d) level; because these were nonstationary points, the projected frequencies were used.

Having identified accurate methods on the basis of the assessment study, these were then used to calculate the free energies of NO–C and N–OC bond homolysis for a large number of alkoxyamines, both in the gas phase and in toluene, at room temperature and at the experimentally relevant temperature of 393.15 K (120 °C). The gas-phase free energies were calculated using the standard textbook formulas for the statistical thermodynamics of an ideal gas under the harmonic oscillator rigid rotor approximation.^{26,27} These calculations were carried out using our in-house program TChem.²⁸ Frequency calculations carried out at the B3-LYP/6-31G(d) level were scaled via the appropriate factors.²⁹ The solution-phase free energies were calculated as the sum of the corresponding gas-phase free energy, the calculated free energy of solvation, and a correction term $RT \ln(RT/P)$, where R is the ideal gas constant, T is the reaction temperature, and P is the standard pressure of 1 atm (101.325 kPa). The correction term takes account of the fact that the solvation energy is computed for the passage from 1 atm (g) to 1 mol L^{−1} (soln).³⁰

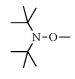
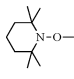
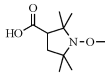
To facilitate direct comparisons between experimental and calculated solution-phase free energies of homolysis, experimental equilibrium constants $K = k_f/k_d$ were obtained by combining independently measured values of the rate coefficients for the forward, k_f , and reverse, k_d , trapping reactions. The experimental free energy was then found from the equation $K = (c)^{\Delta n} \exp(-\Delta G/RT)$, where T is the reaction temperature in Kelvin, R is the ideal gas constant (8.3143 J mol^{−1}K^{−1}), c is the standard unit of concentration (1 mol L^{−1} for the solution-phase data), and Δn is the change in the number of moles on reaction (1 for homolysis).

3. Results and Discussion

3.1. Geometry Optimization. To establish whether differences in the procedure used to optimize molecular geometries will have any significant effect on the calculated energetics of nitroxide reactions, single-point energies in the gas phase were calculated at a consistent level of theory (QCISD/6-31G(d)) for the optimized geometries of various methoxyamines and dissociated products. These energies, with B3-LYP/6-31G(d) frequencies, were used to calculate O–C bond homolysis reaction enthalpies, shown in Table 1. Optimizations were performed using a range of levels of theory from the computationally lower cost Hartree–Fock and density functional theory (DFT) methods to more demanding MP2 and QCISD calculations, with both small and larger basis sets. The results were benchmarked against the QCISD/6-31G(d) method.

In line with previous studies showing that low-cost methods perform very well in geometry optimizations of nitroxides,³¹ all of the lower-cost methods yielded reasonably accurate geometries for the calculation of alkoxyamine dissociation reactions when compared with the benchmark level of theory, though there are some minor differences among the methods used. DFT method B3-LYP/6-31G(d) appears to offer the best compromise between accuracy and computational cost. The enthalpies of homolysis, calculated from geometries optimized at the B3-LYP/6-31G(d) level, show a difference of less than 0.3 kJ mol^{−1} from the corresponding benchmark values. Thus, B3-LYP/6-31G(d) was adopted for the determination of the geometries of molecules in this work.

TABLE 1: Effect of the Level of Theory Used for Geometry Optimization in the Gas-Phase Enthalpy of Homolysis (at 0 K) of Alkoxyamines^a

Level of Theory for the Geometry Optimization	NO–C homolysis enthalpy (kJ mol ^{−1})		
			
HF/6-31G(d)	200.2	206.3	200.0
HF/6-311+G(2d)	200.6	206.3	200.1
HF/6-311+G(3df,2p)	200.5	206.2	199.9
B3-LYP/6-31G(d)	202.9	208.4	202.3
B3-LYP/cc-pVDZ	203.2	208.7	202.4
B3-LYP/6-311+G(2d)	203.0	208.5	202.3
B3-LYP/6-311+G(3df,2p)	203.0	208.5	202.3
B3-LYP/cc-pVTZ	203.0	208.4	202.2
MP2/6-31G(d)	203.6	209.3	202.7
MP2/6-311+G(d)	204.0	209.8	203.0
MP2/6-311+G(3df,2p)	-	210.0	-
QCISD/6-31G(d)	202.9	208.6	-

^a In all cases, homolysis enthalpies were calculated using QCISD/6-31G(d) single-point energies, performed on species optimized using various wave functions and basis sets.

3.2. Gas-Phase Single-Point Energy. To identify an appropriate method for the calculations of gas-phase single-point energies, it would be advantageous to assess various homolysis reactions over a wide variety of levels of theory and compare the results with experimental data. However, at the highest levels of theory, only the calculation of very small systems is possible and corresponding gas-phase experimental data are unavailable for prototypical alkoxyamine homolysis reactions. There are, however, limited experimental data for the gas-phase trapping of some similar systems in the form of experimental heats of formation for the individual reactants and products that make up homolysis reactions forming oxygen- and nitrogen-centered radicals.³² These data points allowed the gas-phase homolysis enthalpies of these reactions to be determined at various high levels of theory and compared directly with experimental results. Calculated and experimental enthalpies of the reactions of small molecular species are shown in Table 2. Calculation methods include very high level method W1U¹¹ as well as high-level composite methods such as CBS-QB3¹² and methods from the G3 family.^{14,15} Enthalpies calculated using the recently reported G4¹³ method were also determined and are included in Table 2. Studies related to this work have shown that this method does not offer significant improvement over the various G3 methods for radical addition and abstraction reactions.³³

Reactions examined in Table 2 include the dissociation of small alkoxyamine H₂NOCH₃ into H₂NO· and ·CH₃ as well as homolysis reactions producing similar small oxygen- and nitrogen-centered radicals. Enthalpies, calculated using the highest theoretical method assessed (W1U), show a mean absolute deviation (MAD) from an experimental value of 3.6 kJ mol^{−1}. The respective MAD for the G3(MP2)-RAD values is only marginally larger, at 5.6 kJ mol^{−1}, despite its considerably lower computational cost. Moreover, for the homolysis reaction forming a methyl radical and oxygen-centered radical H₃CO· (which is most relevant to the present work), the two G3 methods show the smallest deviations from the experimental values. The G3(MP2)-RAD method therefore provides a suitable benchmark level of theory for alkoxyamine homolysis.

TABLE 2: Calculated^a and Experimental^b Enthalpies (298 K) for Gas-Phase Radical-Trapping Reactions

reaction	enthalpy of trapping (kJ mol ⁻¹)					exp.
	CBS-QB3	G3(MP2)-RAD	G3X	G4	W1U	
NH ₃ → H ₂ N [•] + [•] H	447.8	443.0	438.8	441.4	447.9	452.7 ± 1.3
H ₂ NCH ₃ → H ₂ N [•] + [•] CH ₃	357.0	346.8	348.5	350.1	354.8	358.6 ± 2.1
CH ₃ OH → H ₃ CO [•] + [•] H	437.9	435.9	430.3	431.5	438.4	436.0 ± 3.8
H ₃ COCH ₃ → H ₃ CO [•] + [•] CH ₃	356.3	347.5	348.5	347.1	351.5	348.1 ± 4.2
H ₂ NOCH ₃ → H ₂ NO [•] + [•] CH ₃	240.1	237.4	237.0	235.3	237.6	
MAD (kJ mol ⁻¹) ^c	4.1	5.6	7.5	6.3	3.6	0

^a Calculated at various levels of theory using literature-recommended geometries. ^b Taken from ref 32. Where multiple values are provided in this reference, the recommended values are quoted. ^c Mean absolute deviation from experimental values.

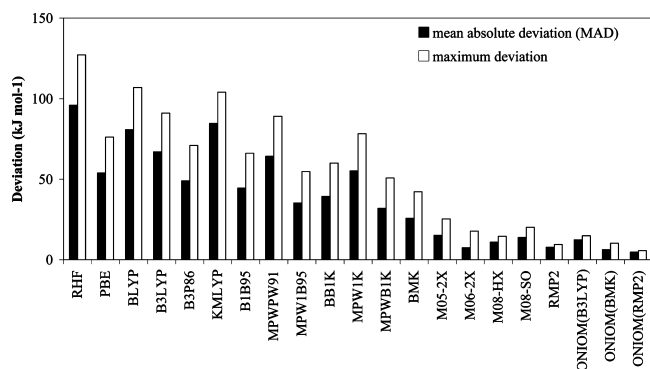


Figure 1. Mean and maximum absolute deviations of various low-cost methods from G3(MP2)-RAD benchmark values for the gas-phase enthalpies of NO–C homolysis (at 0 K) of various TEMPO-alkyl alkoxyamines. Single-point calculations were made with 6-311+G(3df,2p) basis sets for species optimized at the B3-LYP/6-31G(d) level.

Although G3(MP2)-RAD is a relatively computationally efficient high-level composite method, this type of calculation is currently limited to systems of less than around 17 to 18 non-hydrogen atoms using our computational resources. Therefore, suitable lower-cost methods are required for reactions involving larger polymeric and nitroxide radicals. Recently, we have examined the use of various low-cost DFT, MP2, and ONIOM procedures in the calculation of a broad range of radical reactions, including a small test set of alkoxyamine BDEs, with a view to finding a suitable method to use for larger systems for which G3(MP2)-RAD calculations are impractical.⁵ We have now updated the alkoxyamine test set to include calculations using some more recently developed DFT methods (M05-2X, M06-2X, M08-HX, and M08-SO), where a number of these were recently shown to yield improved results for these and/or related reactions.³⁴ A complete set of the results is shown in Figure 1; the corresponding BDEs at the various levels of theory are provided in Table S2 of the Supporting Information.

In Figure 1, it is seen that, in general, the DFT treatments fail to reproduce the G3(MP2)-RAD benchmark enthalpies, having instead large and unpredictable deviations with MADs of over 25 kJ mol⁻¹ and in some cases over 80 kJ mol⁻¹. Consistent with the recent work of Truhlar et al.,³⁴ more success is seen for the newly developed M05-2X, M06-2X, M08-HX, and M08-SO series of DFT methods, with average errors still in the range of 7–15 kJ mol⁻¹. Of these, the M06-2X method showed the best performance for this test set, possibly because these particular reactions were part of the test set used to parametrize this functional. However, even for this functional the maximum error is still 17.8 kJ mol⁻¹. The RMP2 method shows better performance than most of the DFT methods, but the enthalpy values still differ from the benchmark values by

an average of 8 kJ mol⁻¹ and have a maximum deviation of 9.5 kJ mol⁻¹. It is therefore clear that the DFT and RMP2 methods assessed are not suitable as accurate, low-cost methods for reactions in this study.

It has previously been shown that an ONIOM method³⁵ can be used to approximate the G3(MP2)-RAD energies of radical reactions at a much lower computational cost.³⁶ Deviations in homolysis enthalpies of alkoxyamines calculated using ONIOM methods from G3(MP2)-RAD values are shown in Figure 1. In this approach, the full reaction system was calculated using a method such as B3-LYP, BMK, or RMP2 with the 6-311+G(3df,2p) basis set whereas the core system was calculated at G3(MP2)-RAD. The core system was set up to include substituents up to the β position in the nitroxide so that in the core the nitroxide was represented by the small dimethyl nitroxide species, (CH₃)₂NO[•]. In all reactions studied, the use of an ONIOM correction leads to greatly improved results. Thus, for example, at the B3-LYP/6-311+G(3df,2p) level of theory the MAD value decreases from 67.0 to 12.4 kJ mol⁻¹ when the ONIOM correction is applied; for BMK, the MAD value improves from 25.8 to 6.3 kJ mol⁻¹, although the maximum deviation still exceeds 10 kJ mol⁻¹. Not surprisingly, given its performance above, the best results are obtained when the remote substituent effects are measured using RMP2/6-311+G(3df,2p). In this case, the MAD, relative to full G3(MP2)-RAD calculations, is only 4.7 kJ mol⁻¹ and the maximum deviation is only 5.6 kJ mol⁻¹. Therefore, when the computational cost of G3(MP2)-RAD becomes excessive, it is expected that an ONIOM approximation, in which the full nitroxide system is represented by dimethyl nitroxide, will still give a reasonable approximation to the full G3(MP2)-RAD calculated energy.

3.3. Free Energy of Solvation. To assess the level of theory used to calculate free energies of solvation for the species in this work, calculated total free energies of reaction for alkoxyamine homolysis reactions were compared with experimental values found from measured rate constants.^{37–40} Gas-phase energies were calculated at the benchmark G3(MP2)-RAD/B3-LYP/6-31G(d) level and added to free energies of solvation calculated using different levels of theory, basis sets, and solvation models. Because the accuracy of the gas-phase calculation has been separately validated, it was expected that any additional differences would be caused by differences in the free energies of solvation. Three methods of calculating solvation effects were assessed: polarized continuum models PCM¹⁸ and CPCM²¹ and COSMO-RS.²³ Because the experimental measurements were performed at 393 K in *tert*-butyl benzene (*t*BB), the ab initio reaction free energies were also calculated at 393 K in the closely related solvent toluene.

TABLE 3: Effect of the Level of Theory Used for Free Energies of Solvation on the Free Energy (kJ mol⁻¹) of the Homolysis at the NO–C Bond (at 298 K) of Alkoxyamines^a

alkoxyamine	solvation model					exp. ^d
	PCM ^b		CPCM ^b		COSMO-RS ^c	
	HF/6-31G(d)	B3-LYP/6-31G(d)	HF/6-31G(d)	B3-LYP/6-31G(d)	BP86/TZP	
1k	88.2	87.4	87.4	86.2	88.9	90.6
2k	98.0	97.0	97.2	95.9	98.0	101.6
2l	87.0	85.9	85.8	84.6	89.6	87.9
2m	73.8	72.6	72.7	71.3	80.4	66.3
2n	119.0	118.0	118.5	117.2	118.1	123.8
2p	81.5	80.3	80.6	79.2	79.5	78.5
4l	78.9	77.9	77.9	76.6	88.0	89.0
4m	72.5	71.3	71.6	69.9	75.8	72.0
MAD ^e	4.1	4.5	4.4	5.0	4.1	0

^a Incorporating G3(MP2)-RAD//B3-LYP/6-31G(d) gas-phase energies. ^b Calculated using the united atom topological model with the recommended optimization of radii (i.e., UAHF and UAKS keywords for HF/6-31G(d) and B3-LYP/6-31G(d), respectively).²² ^c Geometry not reoptimized in solvent. ^d Calculated from experimental rate constants for homolysis and combination using $K = k_c/k_d$ and $K = \exp(-\Delta G/RT)$. ^e Mean absolute deviation from experimental values.

TABLE 4: Comparison of Calculated and Literature Gas-Phase (298 K) Bond Dissociation Energies (BDEs) (kJ mol⁻¹)

alkoxyamine	PM3 ^a			B3P86/6-311++G(d,p)//B3-LYP/6-31G(d)			G3(MP2)-RAD//B3-LYP/6-31G(d)		
	O–C break	N–O break	diff.	O–C break	N–O break	diff.	O–C break	N–O break	diff.
2a				176 ^a	189 ^a	13	205	231	26
2k	161	107	–54	119 ^a			162	238	76
2l	130	112	–18	108 ^a	174 ^a	66	169	238	69
2m	105	130	25	87 ^a			161	223	62
2o	118			121 ^a	180 ^a	59	182	242	60
2p	86	117	31				169	228	59
2q	142	107	–35	179 ^a	176 ^a	–3	235	237	2
5a				173 ^b	141 ^b	–32	210 ^c	192 ^c	–18
5l				118 ^b	137 ^b	19	195	214	19
5p				102 ^{b,d}	126 ^{b,d}	24	216	226	10
Absolute Values									
MAD ^e	56	118	64	61	65	7	(0)	(0)	(0)
max. deviation ^f	93	131	130	114	100	14	(0)	(0)	(0)
Relative values ^g									
MAD ^e	36	14	51	20	15	8	(0)	(0)	(0)
max. deviation ^f	54	33	59	53	36	17	(0)	(0)	(0)

^a Reference 3. ^b Reference 4. ^c Calculated for model system 5a. ^d Calculated for a C(CH₃)₂CO₂CH₂CH₃ alkyl fragment. ^e Mean absolute deviation from G3(MP2)-RAD values. ^f Maximum deviation from G3(MP2)-RAD values. ^g Relative values calculated using the 2l system as the reference.

The calculated solution-phase free energies for homolysis reactions of a range of alkoxyamines are shown along with the available experimental data^{37–40} in Table 3. As Table 3 shows, there is little variation in the reaction free energies when different methods of calculating the solvation energy are used. The MADs of the calculated free energies from the experimental values vary between 4.1 and 5.0 kJ mol⁻¹. The level of theory, the basis set, and the solvation model have very little effect on the value of the free energy of solvation. As such, the method chosen for the calculation of free energies of solvation in nitroxide trapping reactions appears to be fairly arbitrary for these reactions. The PCM solvation model at the B3-LYP/6-31G(d) level was chosen for further calculations in this study because it gives good solvation energies and has likewise performed well in our studies of the redox potentials of nitroxide radicals^{18,19} while remaining computationally efficient.

3.4. Relative Errors in NO–C and N–OC BDEs. In the assessment study described above, it was found that in order to reproduce experimental free energies for O–C bond homolysis in alkoxyamines high-level composite methods are required. Previous investigations of the competition between NO–C and N–OC in alkoxyamines have been performed using lower-cost semiempirical and B3P86 methods on the basis that these lower

cost methods may be able to describe the qualitative trends in the data.³ It is therefore of interest to see how well these perform against our G3(MP2)-RAD values (Table 4).

From Table 4, it is clear that, as expected, neither of these low-level methods can reproduce the absolute values of the NO–C and N–OC BDEs with MADs in excess of 50 kJ mol⁻¹ and maximum absolute deviations in excess of 100 kJ mol⁻¹. If we next examine the relative values of the BDEs within either the NO–C or N–OC series (taking 2l as our reference in each case), then we note that these errors, while smaller, are still unacceptably large, having MADs ranging from 14 to 36 kJ mol⁻¹ and maximum deviations ranging from 33 to 54 kJ mol⁻¹. Because an error of just 6 kJ mol⁻¹ alters the equilibrium constant by approximately 1 order of magnitude at room temperature, neither of these low levels of theory is suitable for studying substituent effects in these reactions.

Finally, if we instead examine the difference in the NO–C and N–OC BDEs for the same alkoxyamines, then the semiempirical PM3 method still has unacceptably large errors. (For the absolute values, the MAD is 64 kJ mol⁻¹ and the maximum deviation is 130 kJ mol⁻¹.) However, the B3P86 calculations do benefit from some systematic error cancellation and perform reasonably well, with an MAD (for the absolute values) of just

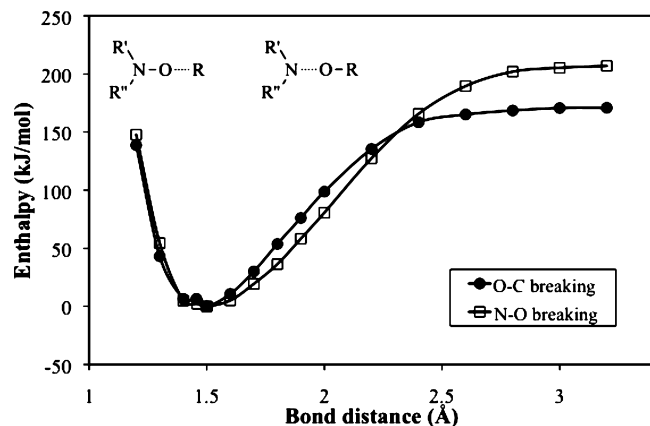


Figure 2. Enthalpy surface (gas phase, 298.15 K) for the homolysis of 1-isopropoxy-2,2,6,6-tetramethyl-piperidine calculated at the MRMP2/6-31G(d)//FORS-MCSCF(2,2)/6-31G(d) level.

7 kJ mol⁻¹, though the maximum deviation is still a little high at 14 kJ mol⁻¹. Moreover, in this case the relative values (i.e., trends) in these values actually have slightly larger levels of error. Although the success of B3P86 in reproducing the NO–C versus N–OC BDE differences is promising and may be improved through the use of more sophisticated DFT methods, for the present work we have retained the use of high-level methods so that both the absolute and relative values of the BDEs that we report are reliable.

3.5. Homolysis Reaction Pathways. Reaction pathways involving the homolysis of a closed-shell species into two radical species usually involve at least two significant configurations (i.e., the bonding and antibonding configurations) and are thus likely to be imperfectly described by a single reference wave function. To calculate the complete reaction pathway accurately, a multireference treatment is therefore usually required. In this case, the minimum description requires an active space including the N–OC (or NO–C) σ bonding and antibonding orbitals along with two active electrons. The multiconfigurational self-consistent field (MCSCF) wave functions were constructed and used to calculate the energies along the path of the homolysis reaction of the alkoxyamine 1-isopropoxy-2,2,6,6-tetramethyl-piperidine (TEMPO–CH(CH₃)₂) into both TEMPO and an isopropyl radical species $\cdot\text{CH}(\text{CH}_3)_2$ and into a 2,2,6,6-tetramethyl-piperidinyl radical and an isopropoxy radical species $\cdot\text{OCH}(\text{CH}_3)_2$.

Figure 2 shows the gas-phase reaction enthalpy curve (298.15 K) of the homolysis of TEMPO–CH(CH₃)₂ at both the O–C and N–O bonds. The active space used for both reactions includes two active electrons and two active orbitals (2, 2) consisting of the σ bonding and σ^* antibonding orbitals of the forming bond. To account for dynamic correlation effects, single-point energies along the path were calculated at the MRMP2/6-31G(d)//FORS-MCSCF(2,2)/6-31G(d) level. The inclusion of lone pairs on the nitrogen and oxygen species into the active space was shown to be unnecessary by a calculation of the O–C breaking homolysis reaction pathway at the MRMP2/6-31G(d)//FORS-MCSCF(8,5)/6-31G(d) level. The MAD of the (2, 2) active space from the (8, 5) active space was only 2.9 kJ mol⁻¹ (Figure S1 in the Supporting Information). The corresponding free energies of homolysis are shown in Figure 3. The extrapolation of these curves to infinity can be compared with the free energies calculated using G3(MP2)-RAD. In the case of the O–C homolysis, the deviations are relatively small (4 kJ mol⁻¹); for N–O homolysis, the deviations are slightly larger (10 kJ mol⁻¹), indicating that a larger basis

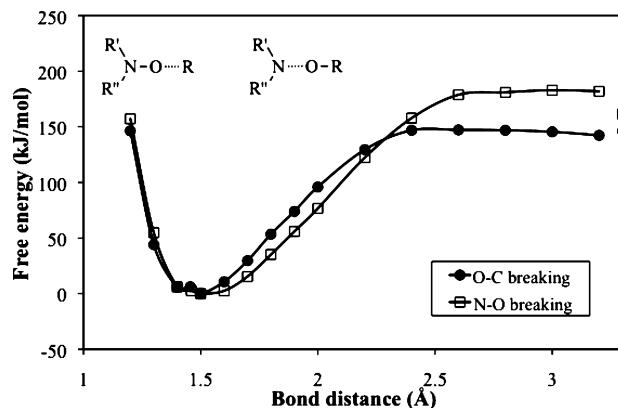


Figure 3. Free-energy surface (298.15 K, gas phase) for the homolysis of 1-isopropoxy-2,2,6,6-tetramethyl-piperidine calculated at the MRMP2/6-31G(d)//FORS-MCSCF(2,2)/6-31G(d) level. The corresponding G3(MP2)-RAD free energies of homolysis are shown on the right y axis for purposes of comparison.

set would be necessary for a chemically accurate treatment of the reaction pathway. Nonetheless, the agreement is close enough to support the use of these curves in a qualitative analysis of the dissociation.

The reaction surface of the O–C and N–O homolysis reactions shown in Figure 2 is a smooth curve, as expected, with no enthalpic barrier. Small free-energy barriers exist because of the effects of entropy, occurring at separations of around 2.6 and 3.0 Å for the O–C and N–O bond-breaking reactions, respectively (Figure 3). However, in general it appears that these effects are minor, at least at synthetically relevant reaction temperatures, and it is the thermochemistry of the process that ultimately determines whether N–OC or NO–C homolysis occurs.

Although the kinetic parameters of the reaction require a multireference treatment, as shown above, single-reference methods such as G3(MP2)-RAD are suitable for calculations of the thermodynamic parameters of these types of trapping reactions. This is because energies of only the reactant and product species are required. The T_1 diagnostic value²⁵ for the TEMPO–CH(CH₃)₂ alkoxyamine is 0.0051, confirming that ground-state alkoxyamine does not require a multireference treatment.

3.6. Structure–Reactivity Trends in Homolysis. Table 5 shows the free energies of homolysis of various alkoxyamines at the NO–C or N–OC bond at 298.15 and 393.15 K with calculations performed both in the gas phase and in toluene. For the TEMPO-based alkoxyamines, we have plotted this difference as a function of the alkyl fragment for each of the sets of reaction conditions (Figure 4). From this Figure (and also the broader data set in Table 5), it is clear that both temperature and the presence of solvent have very little effect on the relative preference for NO–C versus N–OC homolysis.

For the TEMPO series (Figure 4), we see that the NO–C bond is usually most likely to break, and the alternative N–OC dissociation is normally energetically disfavored by more than 50 kJ mol⁻¹. Not surprisingly, the inclusion of substituents (such as phenyl, carbonyl, and cyano) that stabilize the alkyl radical product of NO–C homolysis strongly enhances this preference. At the other extreme, in cases where a heteroatom is present in the position α to the (N–O–C) carbon center, N–OC homolysis becomes the preferred pathway. As discussed in earlier studies of NO–C homolysis, this is because one of the lone pairs on the nitroxyl oxygen lies antiperiplanar to the carbon–heteroatom bond,

TABLE 5: Calculated Gas- and Solution-Phase Free Energies of the Bond Homolysis of NO–C and N–OC Bonds (kJ mol^{−1})^a

alkoxyamine	298 K				393 K			
	gas phase		solution phase (toluene)		gas phase		solution phase (toluene)	
	O–C break	N–O break	O–C break	N–O break	O–C break	N–O break	O–C break	N–O break
1a	144.5	152.5	155.3	158.4	127.1	132.3	146.1	146.0
1f	162.2	144.2	166.2	148.1	143.2	123.5	154.4	137.2
1g	183.4	146.0	190.4	150.5	164.4	126.0	178.9	138.1
1k ^b	99.5	157.3	97.8	155.5	81.7	136.7	87.4	142.2
1l ^b	90.1	148.7	84.4	145.6	69.3	127.2	71.1	132.0
1o ^b	107.1	155.1	103.3	153.9	86.5	133.3	90.2	140.0
1p ^b	90.0	140.3	84.9	137.5	68.3	118.3	71.8	123.4
1q ^b	160.0	152.3	155.5	150.1	139.5	131.4	142.4	136.7
1r	145.5	146.9	148.1	148.8	124.6	125.5	134.9	135.3
1s ^b	103.5	153.6	101.4	153.0	82.9	131.9	88.3	138.8
1t	115.9	146.3	112.7	147.2	95.1	125.0	99.8	133.2
2a	151.8	169.7	162.3	174.9	134.7	150.3	153.4	163.2
2b	155.3	167.8	159.3	169.4	135.4	146.9	148.1	157.5
2c	158.6	172.9	158.9	173.6	139.3	153.7	146.5	161.9
2d	146.1	161.6	147.5	161.8	124.8	141.1	134.1	149.5
2e	132.3	143.1	132.9	142.7	111.8	123.0	121.0	131.2
2f	168.5	160.3	172.9	164.2	149.1	139.9	160.9	153.7
2g	190.1	162.6	197.6	167.2	171.0	143.0	186.1	155.3
2h	119.7	183.3	126.7	185.7	102.3	164.2	117.0	174.0
2i	115.3	180.2	115.7	181.2	95.3	160.0	103.4	169.3
2j ^b	93.1	162.3	91.6	162.2	72.0	141.3	79.0	149.7
2k ^b	108.7	176.7	107.0	174.5	91.5	157.1	97.0	162.1
2l ^b	105.0	173.8	98.8	169.7	84.7	153.3	86.0	157.1
2m ^b	92.7	154.9	86.0	150.2	70.9	139.8	72.6	143.8
2n ^b	129.1	177.1	129.2	175.4	110.7	156.7	118.0	162.5
2o ^b	118.3	176.4	113.5	173.9	98.2	155.7	100.7	160.8
2p ^b	99.7	160.2	93.6	156.0	77.9	138.7	80.3	142.2
2q ^b	169.3	171.8	164.3	168.7	148.5	151.1	150.8	155.3
2r	156.1	167.4	158.4	168.6	135.7	147.0	145.6	156.0
2s ^b	115.0	175.3	112.2	173.6	95.1	154.8	99.7	160.5
2t ^b	130.7	171.2	126.6	170.9	111.0	151.5	114.6	158.2
3a	140.8	157.8	150.2	160.6	124.3	140.1	141.6	150.1
3f	165.5	156.3	168.2	157.5	146.4	137.2	156.2	147.7
3g	183.6	155.1	189.1	156.7	164.2	136.4	177.1	145.0
3l ^b	96.8	168.7	87.2	160.1	76.8	149.7	73.8	147.8
3o ^b	110.6	171.9	102.8	165.3	90.8	152.6	89.7	152.7
3p ^b	92.2	155.9	83.8	148.2	70.2	135.3	69.8	134.6
3q ^b	158.6	164.2	151.4	157.9	137.7	144.6	137.2	144.7
3r	156.3	166.5	155.6	163.8	136.2	147.5	142.5	151.7
3s ^b	108.8	172.2	103.1	166.6	89.1	153.1	90.2	153.9
3t ^b	120.4	164.1	116.2	162.5	100.9	145.8	104.3	150.8
4a	142.4	158.2	152.3	161.4	125.6	140.2	143.5	150.8
4f	166.7	156.4	170.0	157.8	147.2	136.9	157.7	147.9
4g	183.8	154.2	189.7	155.8	164.5	135.5	177.7	144.3
4l ^b	100.2	171.4	91.0	162.9	80.6	152.7	77.9	151.0
4m ^b	92.9	157.6	85.1	150.4	71.1	143.5	71.3	144.5
4o ^b	110.8	171.4	103.8	165.3	91.1	152.1	90.7	152.8
4p ^b	92.8	155.7	86.4	149.7	70.6	134.8	72.0	135.8
4q ^b	161.6	166.4	155.4	160.8	141.0	147.1	141.7	148.2
4r ^b	146.8	167.9	144.2	162.8	126.8	148.9	130.4	150.2
4s ^b	108.3	171.0	103.4	165.7	88.4	151.6	90.3	153.1
4t ^b	121.3	164.3	117.0	162.3	101.4	145.5	104.6	150.2
5a ^b	156.6	131.3	139.6	112.1	164.7	131.3	155.5	119.3
5l ^c	132.4	152.3	112.6	132.4	119.4	138.8	106.2	125.6
5p ^c	142.1	153.7	118.6	130.7	127.5	138.3	112.2	122.5

^a G3(MP2)-RAD//B3-LYP/6-31G(d) values except where noted with the free energy of solvation calculated using PCM at the B3-LYP/6-31G(d) level using the united atom topological model with the recommended optimization of radii (UAKS keyword in Gaussian). ^b ⁱONIOM approximation of G3(MP2)-RAD//B3-LYP/6-31G(d) values including (CH₃)₂NO-alkyl in the core system, with the full system calculated at the RMP2/6-311+G(3df,2p) level. ^c ONIOM approximation of G3(MP2)-RAD//B3-LYP/6-31G(d) values including (Me)₂NOR in the core system, 1-alkyl-2,2-dimethylindoline as the middle system calculated at the RMP2/6-311+G(3df,2p) level, and the full system calculated at the RMP2/6-311+G(2d) level.

allowing hyperconjugation to occur between the lone pair and the σ^* antibonding orbital of the bond.^{3,17,41,42} This anomeric stabilization results in a significant lengthening of the NOC–heteroatom bond whereas the NO–C bond is significantly shortened and strengthened. It is expected that

when anomeric stabilization of the alkoxyamine occurs, nitroxide-mediated polymerization will be less effective because of the N–OC homolysis side reaction.

To examine the effect of nitroxide structure, Figure 5 shows a plot of the free energies of NO–C and N–OC homolysis for

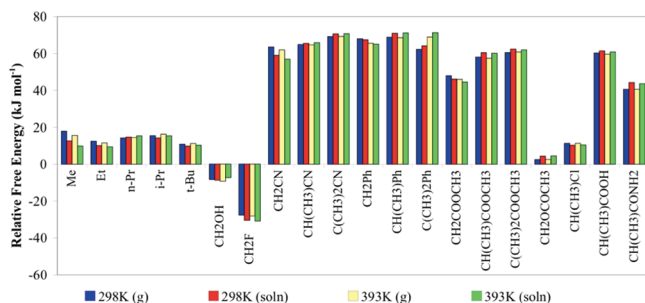


Figure 4. Relative free energies (kJ mol^{-1}) for N-OR versus NO-R homolysis at 393 K in toluene as a function of R for the series of TEMPO-based alkoxyamines. A positive free-energy difference indicates that the NO-R homolysis is favored. Data for the gas and solution (toluene) phases are shown at 298 and 393 K.

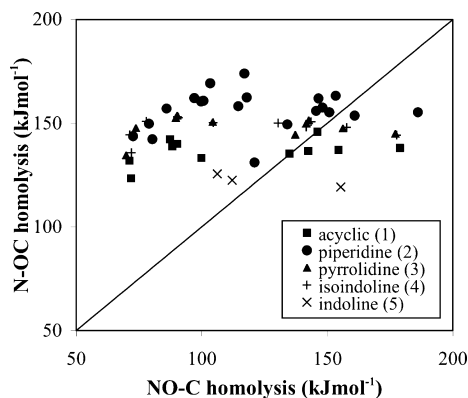


Figure 5. Free energies (393 K in toluene) of NO-C and N-OC bond homolysis for the test set of alkoxyamines.

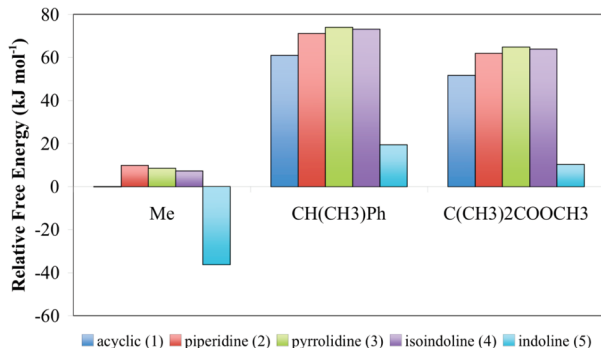


Figure 6. Relative free energies (kJ mol^{-1}) for N-OR versus NO-R homolysis at 393 K in toluene for combinations of $R = \text{Me}$, $\text{CH}(\text{CH}_3)\text{Ph}$, and $\text{C}(\text{CH}_3)_2\text{COOCH}_3$ and nitroxide structures 1–5 in Scheme 3. A positive free-energy difference indicates that the NO-R homolysis is favored.

the complete data set at the experimentally relevant condition of 393 K in toluene. From this Figure, it is clear that NO-C and N-OC homolysis are not correlated. Whereas NO-C homolysis can be successfully modeled in terms of the polar and radical stabilization terms describing the individual alkyl and nitroxide radicals,¹⁷ when this same free-energy relationship is applied to the N-OC bond homolysis in the present work the fit is extremely poor ($R^2 = 0.05$). Instead, the N-OC homolysis appears to be much more dependent upon the stability of the released aminyl radical. To examine this further, Figure 6 shows the effect of the nitroxide structure on the relative free energies of homolysis of the NO-C or N-OC bond at 393.15 K in toluene for three different alkyl groups, $R = \text{Me}$, $\text{CH}(\text{CH}_3)\text{Ph}$, and $\text{C}(\text{CH}_3)_2\text{COOCH}_3$. In each case, the indoline derivative shows the greatest relative preference for N-OC

homolysis because of the resonance stabilization of the released aminyl radical. In absolute terms, the N-OC homolysis is still favored only for certain R groups (e.g., $R = \text{CH}_3$ in the systems examined), but in all cases, the N-OC bond dissociation energy is greatly reduced. The only other notable trend is that the acyclic species consistently has slightly lower relative N-OC bond dissociation energies than the remaining cyclic compounds, presumably because its resulting aminyl radical is more easily pyramidalized at nitrogen.

4. Conclusions

The competition of NO-C and N-OC homolysis in various alkoxyamines was investigated using high-level computational methods. It was found that the free energies of NO-C and N-OC homolysis are not correlated, with NO-C homolysis being more dependent upon the properties of the alkyl fragment and N-OC homolysis being more dependent upon the structure of the aminyl fragment. For piperidine-, pyrrolidine-, and isoindoline-based nitroxides, N-OC homolysis is favored above NO-C homolysis only in the case where a heteroatom that is α to the NOC carbon center stabilizes the NO-C bond, though it may become a competitive minor reaction for primary alkyl radicals. Acyclic and indoline-type species have lower free energies of N-OC homolysis than other cyclic species because of the greater stability of the aminyl radical fragment and are less resistant to this unwanted side reaction.

As part of this work, a series of assessment studies were used to determine appropriate levels for the calculation of alkoxyamine homolysis reactions. It was determined that G3(MP2)-RAD//B3-LYP/6-31G(d) is an appropriate level of theory for the calculation of gas-phase reactions and molecular properties, with an ONIOM approximation to G3(MP2)-RAD (in which the full system is calculated at the RMP2/6-311+G(3df,2p) level of theory) providing good results for large systems. For reactions calculated in solution, the effects of the solvent medium are well described by a PCM method at the B3-LYP/6-31G(d) level. Using these methods, deviations between calculated values of alkoxyamine homolysis reactions and available experimental results are around 5 kJ mol^{-1} . On the basis of this, chemical accuracy is achieved.

Acknowledgment. This research was undertaken on the NCI National Facility in Canberra, Australia, which is supported by the Australian Commonwealth Government. We gratefully acknowledge support (to M.L.C) from the Australian Research Council under their Centres of Excellence program and the award (to J. L. H.) of an Australian Postgraduate Award and an O'Donnell Young Scientist Prize from the RACI Polymer Division. M.S.G. and L.B.R. acknowledge the support of the U.S. Air Force Office of Scientific Research.

Supporting Information Available: B3-LYP/6-31G(d)-optimized geometries in the form of Gaussian archive entries, corresponding total energies, thermal corrections, entropies, free energies, and data used to construct to Figure 1. This material is available free of charge via the Internet at <http://pubs.acs.org>.

References and Notes

- Allen, N. S. *Chem. Soc. Rev.* **1986**, *15*, 373.
- Hodgson, J. L.; Coote, M. L. *Macromolecules* **2010**, *43*, 4573.
- Gaudel-Siri, A.; Siri, D.; Tordo, P. *ChemPhysChem* **2006**, *7*, 430.
- Gigmes, D.; Gaudel-Siri, A.; Marque, S. R. A.; Bertin, D.; Tordo, P.; Astolfi, P.; Greci, L.; Rizzoli, C. *Helv. Chim. Acta* **2006**, *89*, 2312.
- Izgorodina, E. I.; Brittain, D. B. R.; Hodgson, J. L.; Krenke, E. H.; Lin, C. Y.; Namazian, M.; Coote, M. L. *J. Phys. Chem. A* **2007**, *111*, 10754.

- (6) Hehre, W. J.; Radom, L.; Schleyer, P. V. R.; Pople, J. A. *Ab Initio Molecular Orbital Theory*; Wiley: New York, 1986.
- (7) Koch, W.; Holthausen, M. C. *A Chemist's Guide to Density Functional Theory*; Wiley-VCH: Weinheim, Germany, 2000.
- (8) Frisch, M. J.; Trucks, G. W.; Schlegel, H. B.; Scuseria, G. E.; Robb, M. A.; Cheeseman, J. R.; Montgomery Jr., J. A.; Vreven, T.; Kudin, K. N.; Burant, J. C.; Millam, J. M.; Iyengar, S. S.; Tomasi, J.; Barone, V.; Mennucci, B.; Cossi, M.; Scalmani, G.; Rega, N.; Petersson, G. A.; Nakatsuji, H.; Hada, M.; Ehara, M.; Toyota, K.; Fukuda, R.; Hasegawa, J.; Ishida, M.; Nakajima, T.; Honda, Y.; Kitao, O.; Nakai, H.; Klene, M.; Li, X.; Knox, J. E.; Hratchian, H. P.; Cross, J. B.; Adamo, C.; Jaramillo, J.; Gomperts, R.; Stratmann, R. E.; Yazyev, O.; Austin, A. J.; Cammi, R.; Pomelli, C.; Ochterski, J. W.; Ayala, P. Y.; Morokuma, K.; Voth, G. A.; Salvador, P.; Dannenberg, J. J.; Zakrzewski, V. G.; Dapprich, S.; Daniels, A. D.; Strain, M. C.; Farkas, O.; Malick, D. K.; Rabuck, A. D.; Raghavachari, K.; Foresman, J. B.; Ortiz, J. V.; Cui, Q.; Baboul, A. G.; Clifford, S.; Cioslowski, J.; Stefanov, B. B.; Liu, G.; Liashenko, A.; Piskorz, P.; Komaromi, I.; Martin, R. L.; Fox, D. J.; Keith, T.; Al-Laham, M. A.; Peng, C. Y.; Nanayakkara, A.; Challacombe, M.; Gill, P. M. W.; Johnson, B.; Chen, W.; Wong, M. W.; Gonzalez, C.; Pople, J. A. *Gaussian 03*, revision B.03; Gaussian, Inc.: Pittsburgh PA, 2003.
- (9) Werner, H.-J.; Knowles, P. J.; Amos, R. D.; Bernhardsson, A.; Berning, A.; Celani, P.; Cooper, D. L.; Deegan, M. J. O.; Dobbyn, A. J.; Eckert, F.; Hampel, C.; Heter, G.; Korona, T.; Lindh, R.; Lloyd, A. W.; McNicholas, S. J.; Manby, F. R.; Meyer, W.; Mura, M. E.; Nicklass, A.; Palmieri, P.; Pitzer, R.; Rauhut, G.; Schütz, M.; Stoll, H.; Stone, A. J.; Tarroni, R.; Thorsteinsson, T. MOLPRO 2000.6; University of Birmingham: Birmingham, England, 1999.
- (10) (a) Schmidt, M. W.; Baldridge, K. K.; Boatz, J. A.; Elbert, S. T.; Gordon, M. S.; Jensen, J. H.; Koseki, S.; Matsunaga, N.; Nguyen, K. A.; Su, S.; Windus, T. L.; Dupuis, M.; Montgomery, J. A. *J. Comput. Chem.* **1993**, *14*, 1347. (b) Gordon, M. S.; Schmidt, M. W. In *Theories and Applications of Computational Chemistry: The First Forty Years*; Dykstra, C. E., Frenking, G., Kim, K. S., Scuseria, G. E., Eds.; Elsevier: Amsterdam, 2005; pp 1167–1189.
- (11) Martin, J. M. L.; de Oliveira, G. J. *J. Chem. Phys.* **1999**, *111*, 1843.
- (12) Montgomery Jr., J. A.; Frisch, M. J.; Ochterski, J. W.; Petersson, G. A. *J. Chem. Phys.* **2000**, *112*, 6532.
- (13) Curtiss, L. A.; Redfern, P. C.; Raghavachari, K. *J. Chem. Phys.* **2007**, *126*, 084108.
- (14) Curtiss, L. A.; Raghavachari, K. *Theor. Chem. Acc.* **2002**, *108*, 61.
- (15) Henry, D. J.; Sullivan, M. B.; Radom, L. *J. Chem. Phys.* **2003**, *118*, 4849.
- (16) Vreven, T.; Morokuma, K. *Theor. Chem. Acc.* **2003**, *109*, 125.
- (17) Hodgson, J. L.; Lin, C. Y.; Coote, M. L.; Marque, S. R. A.; Matyjaszewski, K. *Macromolecules* **2010**, *43*, 3728.
- (18) Blinco, J. P.; Hodgson, J. L.; Morrow, B. J.; Walker, J. R.; Will, G. D.; Coote, M. L.; Bottle, S. E. *J. Org. Chem.* **2008**, *73*, 6763.
- (19) Hodgson, J. L.; Namazian, M.; Bottle, S. E.; Coote, M. L. *J. Phys. Chem. A* **2007**, *111*, 13595.
- (20) (a) Cancès, M. T.; Mennucci, B.; Tomasi, J. *J. Chem. Phys.* **1997**, *107*, 3032. (b) Cossi, M.; Barone, V.; Mennucci, B.; Tomasi, J. *Chem. Phys. Lett.* **1998**, *286*, 253. (c) Mennucci, B.; Tomasi, J. *J. Chem. Phys.* **1997**, *106*, 5151.
- (21) (a) Barone, V.; Cossi, M. *J. Phys. Chem. A* **1998**, *102*, 1995. (b) Cossi, M.; Rega, N.; Scalmani, G.; Barone, V. *J. Comput. Chem.* **2003**, *24*, 669.
- (22) Frisch, A.; Frisch, M. J.; Trucks, G. W. *Gaussian 03 User's Reference*; Gaussian, Inc.: Wallingford, CT, 2003.
- (23) (a) Klamt, A. *COSMO-RS: From Quantum Chemistry to Fluid Phase Thermodynamics and Drug Design*; Elsevier Science Ltd.: Amsterdam, 2005. (b) Klamt, A.; Jonas, V.; Burger, T.; Lohrenz, J. C. W. *J. Phys. Chem. A* **1998**, *102*, 5074. (c) Klamt, A. *J. Phys. Chem.* **1995**, *99*, 2224.
- (24) (a) te Velde, G.; Bickelhaupt, F. M.; van Gisbergen, S. J. A.; Fonseca Guerra, C.; Baerends, E. J.; Snijders, J. G.; Ziegler, T. *J. Comput. Chem.* **2001**, *22*, 931. (b) Fonseca Guerra, C.; Snijders, J. G.; te Velde, G.; Baerends, E. *J. Theor. Chem. Acc.* **1998**, *99*, 391. (c) ADF 2008.01, COSMO-RS.SCM. Available via the Internet at www.scm.com.
- (25) Lee, T. J.; Taylor, P. R. *Int. J. Quant. Chem. Symp.* **1989**, *23*, 199.
- (26) See, for example, (a) Stull, D. R.; Westrum, E. F., Jr.; Sinke, G. C. *The Thermodynamics of Organic Compounds*; John Wiley & Sons: New York, 1969. (b) Robinson, P. J. *J. Chem. Educ.* **1978**, *55*, 509–510. (c) Steinfeld, J. I.; Francisco, J. S.; Hase, W. L. *Chemical Kinetics and Dynamics*; Prentice Hall: Englewood Cliffs, NJ, 1989.
- (27) These formulae are outlined in full in the Supporting Information of an earlier publication: Coote, M. L.; Radom, L. *Macromolecules* **2004**, *37*, 590.
- (28) This program is freely available from <http://rsc.anu.edu.au/~cylin/scripts.html>. For more details, see Lin, C. Y.; Izgorodina, E. I.; Coote, M. L. *J. Phys. Chem. A* **2008**, *112*, 1956.
- (29) Scott, A. P.; Radom, L. *J. Phys. Chem.* **1996**, *100*, 16502.
- (30) Liptak, M. D.; Gross, K. G.; Seybold, P. G.; Feldgus, S.; Shields, G. C. *J. Am. Chem. Soc.* **2002**, *124*, 6421.
- (31) Siri, D.; Gaudel-Siri, A.; Tordo, P. *J. Mol. Struct.: THEOCHEM* **2002**, *582*, 171.
- (32) Luo, Y.-R. *Handbook of Bond Dissociation Energies in Organic Compounds*; CRC Press: Boca Raton, FL, 2003.
- (33) Lin, C. Y.; Hodgson, J. L.; Namazian, M.; Coote, M. L. *J. Phys. Chem. A* **2009**, *113*, 3690.
- (34) (a) Zhao, Y.; Truhlar, D. G. *Acc. Chem. Res.* **2008**, *41*, 157. (b) Zhao, Y.; Schultz, N. E.; Truhlar, D. G. *J. Chem. Theory Comput.* **2006**, *2*, 364. (c) Zhao, Y.; Truhlar, D. G. *J. Phys. Chem. Lett.* **2008**, *112*, 1095. (d) Zhao, Y.; Truhlar, D. G. *J. Chem. Theory Comput.* **2008**, *4*, 1849.
- (35) Humbel, S.; Sieber, S.; Morokuma, K. *J. Chem. Phys.* **1996**, *105*, 1959.
- (36) Izgorodina, E. I.; Coote, M. L. *J. Phys. Chem. A* **2006**, *110*, 2486.
- (37) Marque, S. R. A.; Le Mercier, C.; Tordo, P.; Fischer, H. *Macromolecules* **2000**, *33*, 4402.
- (38) Beckwith, A. L. J.; Bowry, V. W.; Ingold, K. U. *J. Am. Chem. Soc.* **1992**, *114*, 4983.
- (39) Sobek, J.; Martschke, R.; Fischer, H. *J. Am. Chem. Soc.* **2001**, *123*, 2849.
- (40) Fischer, H.; Marque, S. R. A.; Nesvadba, P. *Helv. Chim. Acta* **2006**, *89*, 2330.
- (41) Ciriano, M. V.; Korth, H.-G.; van Scheppingen, W. B.; Mulder, P. *J. Am. Chem. Soc.* **1999**, *121*, 6375.
- (42) Marque, S. R. A.; Fischer, H.; Baier, E.; Studer, A. *J. Org. Chem.* **2001**, *66*, 1146.

JP1064165